# Climatic control of the high-latitude vegetation greening trend and Pinatubo effect

Wolfgang Lucht, Ian Colin Prentice, Ranga B Myneni, Stephen Sitch, Pierre Friedlingstein, Wolfgang Cramer, Philippe Bousquet, Wolfgang Buermann, Benjamin Smith

# Climatic Control of the High-Latitude Vegetation Greening Trend and Pinatubo Effect

**Wolfgang Lucht,[1*] I. Colin Prentice,[2] Ranga B. Myneni,[3] Stephen Sitch,[1] Pierre Friedlingstein,[4] Wolfgang Cramer,[1] Philippe Bousquet,[4] Wolfgang Buermann,[3] Benjamin Smith[5]**

**A biogeochemical model of vegetation using observed climate data predicts the high northern latitude greening trend over the past two decades observed by satellites and a marked setback in this trend after the Mount Pinatubo volcano eruption in 1991. The observed trend toward earlier spring budburst and in-creased maximum leaf area is produced by the model as a consequence of biogeochemical vegetation responses mainly to changes in temperature. The post-Pinatubo decline in vegetation in 1992–1993 is apparent as the effect of temporary cooling caused by the eruption. High-latitude $CO_2$ uptake during these years is predicted as a consequence of the differential response of heterotrophic respiration and net primary production.**

Satellite observations over the past two decades indicate a trend toward longer growing seasons and greater annual net primary production (NPP) in high latitudes (*1*–*3*). Using a dynamic vegetation model that predicts leaf area index (LAI), primary production, and net ecosystem carbon exchange from first principles (*4*–*7*), we show that the trend and variability in the satellite observations are consistent quantitatively with independent climate data and qualitatively with net ecosystem carbon exchange, which was independently calculated from atmospheric $CO_2$ concentration measurements (*8*).

We analyzed data for a 1982–1998 interval for which we had access to both climate and satellite data. A previous analysis of 10 years of data from the Advanced Very High Resolution Radiometer (AVHRR) indicated a progressive greening of the boreal zone. A steady increase in annual maximum LAI during 1981–1991 was associated with a slight advance of spring budburst and delay of autumn abscission (*1*). Subsequent work spanning 1981–1999 has confirmed these findings (*2*, *9*), but doubts about the validity of the trend have persisted because of the need for data corrections for instrumental and navigational drift, intercalibration of successive instruments, and consideration of aerosol effects (*10*). Such doubts could be dispelled if the interannual variations in greenness and growing season length were shown to be quantitatively consistent with independent expectations on the basis of climate variability and/or with independent reconstructions of changes in regional $CO_2$ balance. This analysis uses a climate-driven terrestrial carbon cycle model capable of simulating the interannual variability of LAI and the components of the terrestrial carbon balance.

We compare monthly LAI anomalies for the boreal zone, derived from a recent version of the AVHRR data, with monthly LAI anomalies independently predicted by the LPJ Dynamic Global Vegetation Model (LPJ-DGVM), a biogeochemical process model driven by monthly climate observations and by the global mean $CO_2$ concentration increase (see Materials and Methods in supporting online material). Both simulated and observed LAI anomalies show an overall increasing trend, but periods lasting several years with positive or negative deviations from the trend can be discerned in the observations and are correctly simulated (Fig. 1). The pattern of LAI anomalies within each year is, in general, correctly simulated, although discrepancies are seen in 1988 and 1996. The similarity between the model results and the observations is seen not only for the whole boreal zone but also for each separate continent, even though the patterns differ substantially among the continents.

Further analysis of the data and model results (Fig. 2) reveals an increasing trend in the annual maximum LAI during 1982–1991 (+0.23, observed), an abrupt decline from 1991–1992, and a resumed increase during 1992–1998 (+0.19). The model reproduces 65% of the amplitude of the increasing trend before 1992, 85% of the trend after 1992, and 63% of the overall trend (table S1). According to the AVHRR data, the overall greening trend is associated with an advance of spring budburst by several days and a similar delay of autumn leaf-fall (Fig. 2). The model agrees closely with the trend in spring onset and its interannual variability ($r = 0.91$), and it also shows a delay in autumn onset. The amplitude of this delay is underestimated, but this quantitative comparison is less appropriate than for spring onset because the model estimates the timing of cessation of carbon assimilation rather than the timing of leaf abscission, which is what is visible from space.

During the analysis period, global average $CO_2$ concentration rose by 25 parts per million (ppm), annual mean temperature in the boreal zone increased by 0.8 K, and annual precipitation increased by 9.7 mm. Individually, each of these changes would be expected to increase NPP. The model showed boreal zone NPP increasing by 34.6 gC/m$^2$/year (where gC is grams of carbon) and heterotrophic respiration by 31.7 gC/m$^2$/year (linear trends), which is an imbalance of −2.9 gC/m$^2$/year (the minus sign denotes uptake from the atmosphere, i.e., a terrestrial carbon sink). When taking into account the modeled burning of biomass, the magnitude of the sink is increased to −3.6 gC/m$^2$/year (−0.1 PgC/year for the region). The average overall modeled sink for the period is −7.8 gC/m$^2$/year (−0.2 PgC/year).

To determine the climatic factors leading to the observed trends and variability, we ran the vegetation model while keeping selected climatic inputs constant at 1966–1995 average values. We find that variations in temper-

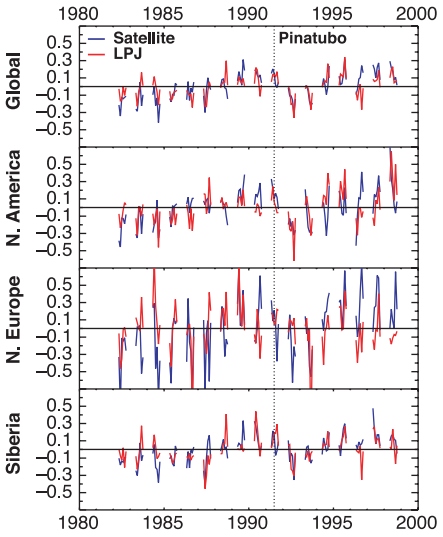


**Fig. 1.** Monthly boreal zone anomalies of LAI from the AVHRR satellite time series and simulated with the LPJ-DGVM. Due to the low solar angle and snow cover during the winter, only growing season anomalies (May to October) were evaluated. Dotted vertical line indicates time of Pinatubo event.

[1]Potsdam Institute for Climate Impact Research, Post Office Box 601203, D–14412 Potsdam, Germany. [2]Max Planck Institute for Biogeochemistry, Post Office Box 100164, D–07745 Jena, Germany. [3]Department of Geography, Boston University, Boston, MA 02215, USA. [4]Laboratoire des Sciences du Climat et de'l Environment, F–91198 Gif-sur-Yvette Cedex, France. [5]Department of Physical Geography and Ecosystems Analysis, Lund University, S-22362 Lund, Sweden.

*To whom correspondence should be addressed. E-mail: Wolfgang.Lucht@pik-potsdam.de

ature alone account for nearly all of the modeled behavior. Changes in precipitation and physiological effects of atmospheric $CO_2$ concentration contribute only marginally (Figs. 2 and 3).

Stratospheric aerosol generated by the Pinatubo eruption in 1991 depressed incoming short-wave radiation. The global effect was still $\approx -1$ W/m$^2$ even a year after the event (*11*, *12*). As a result, an anomalous cooling of $\approx -0.5$ K was observed (*13*) in the northern high-latitude growing seasons of 1992–1993. The AVHRR data indicate a large negative anomaly of LAI in the boreal zone during these years. The reliability of this finding, taken in isolation, is uncertain because volcanic aerosols increase atmospheric scattering and could have spuriously lowered the apparent LAI. However, the LAI values estimated from the satellite data agree closely with those we simulate from climate data during this period (Fig. 2). Both data and model results indicate that the northern biosphere suffered an abrupt setback (*9*) after 1991, followed by a resumption of the greening trend in 1993. The decline in LAI from 1991 to 1992 was 0.27 in the satellite data and 0.22 in the model results. Spring onset was delayed by four days according to the satellite data and three days in the model. Autumn onset was brought forward by nine days according to the satellite data and four days in the model. These reactions to the Pinatubo eruption occurred more or less uniformly on all three northern continents (Fig. 1).

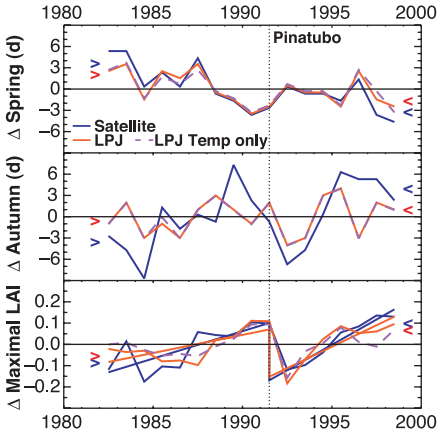


**Fig. 2.** Relative changes in boreal zone timing of spring green-up and autumn senescence, and anomalies of maximal LAI, from the AVHRR satellite time series (blue) and simulated with the LPJ-DGVM (red). Markings on either side of the curves indicate the starting and ending points of linear fits to the whole time period. The LAI is shown to display a break of linear trends in 1991, the year in which the volcano Mount Pinatubo erupted. Results for LPJ-DGVM simulations with constant atmospheric carbon dioxide concentration, precipitation, and cloudiness (1966–1995 averages) but variable observed temperatures are given for comparison (purple dashed line).

The agreement of satellite data and model results suggests that the LAI setback seen in the satellite data during 1992–1993 represents the response of the biosphere to the Pinatubo cooling event. Furthermore, simulated net primary production was reduced by 21.5 gC/m$^2$ and simulated heterotrophic (soil microbial) respiration was reduced by 32.2 gC/m$^2$. When variability in natural biomass burning (a small but significant contribution to the overall carbon balance of boreal ecosystems) is also accounted for, the modeled effect of the Pinatubo anomaly is to increase the boreal zone carbon sink (excluding agricultural lands) by −0.17 PgC/year compared with the 17-year average. The modeled occurrence of an enhanced sink in the years immediately after the Pinatubo event agrees qualitatively with numerical inversion results (*8*) based on spatial patterns of measured atmospheric $CO_2$ concentrations in the remote troposphere (Fig. 3). The climate-driven model results and the inversion results agree that boreal zone carbon exchange anomalies before 1992 were neutral or positive, whereas an anomalous sink developed in 1992–1993. A difference in the magnitude of net ecosystem exchange (NEE) and its anomalies between the model and the inversion is possibly caused in the former by remaining uncertainty in the temperature dependence of respiration; the latter, however, is not fully robust for the boreal region due to the sparsity of the $CO_2$ observation network at high northern latitudes, potentially leading to influence from adjacent temperate regions. The unbalanced effect of cooling on NPP and microbial respiration provides a more simple explanation for additional high-latitude $CO_2$ uptake than a proposed mechanism of increased NPP due to an increase in diffuse sky light (*14*). Our findings support the suggestion (*15*) that the effects of cooling in the boreal zone contributed to the reduction in the growth rate of the global atmospheric $CO_2$ concentration during 1992–1993 (*16*).

We conclude that there has been a greening trend in the high northern latitudes, associated with a gradual lengthening of the growing season [which has also been shown by additional evidence such as tree phenology trends (*17*) and reduced snow cover extent (*18*)], caused by a slight warming of boreal climate during the past two decades. The trend cannot easily be explained away as an artifact of the methods used to calibrate long satellite time series. The trend was dramatically interrupted by the Pinatubo eruption, which reduced LAI while producing an increased carbon sink that contributed to the observed (and temporary) slowdown in the global rate of atmospheric $CO_2$ concentration growth (*19*). Understanding the causes of such variability is an important step in distinguishing natural from human-induced perturbations of Earth's ecosystems.

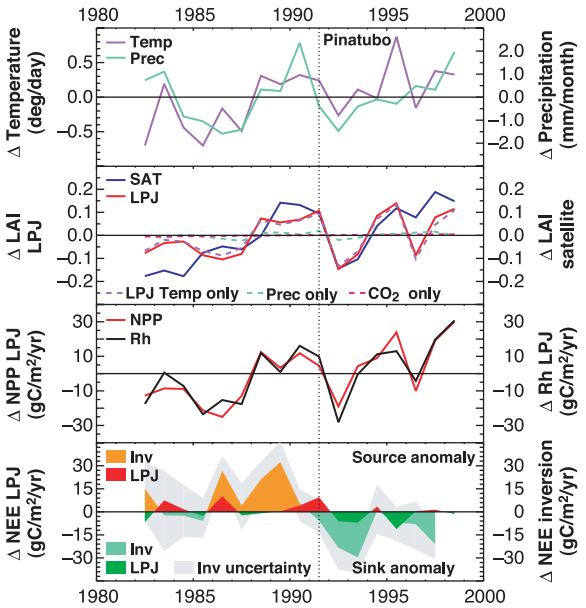


**Fig. 3.** Global boreal zone anomalies of climate (University of East Anglia monthly climatology), LAI (AVHRR satellite time series and LPJ-DGVM simulations), NPP and soil respiration (LPJ-DGVM simulations), and NEE of carbon (LPJ-DGVM simulations and inversions of observations of atmospheric $CO_2$ concentration). For comparison, results are given of LPJ-DGVM simulations allowing only temperature (purple dashed line), precipitation (green dashed line), or atmospheric $CO_2$ concentration (red dashed line) to vary while other climatic inputs were kept constant at 1966–1995 average values.


**References and Notes**

1. R. B. Myneni, C. D. Keeling, C. J. Tucker, G. Asrar, R. R. Nemani, *Nature* **386**, 698 (1997).
2. R. B. Myneni *et al.*, *Proc. Natl. Acad. Sci. U.S.A.* **98**, 14784 (2001).
3. L. Zhou *et al.*, *J. Geophys. Res.* **106**, 20069 (2001).
4. S. Sitch, thesis, Lund University, Sweden (2000).
5. W. Cramer *et al.*, *Global Change Biol.* **7**, 357 (2001).
6. D. McGuire *et al.*, *Global Biogeochem. Cycles* **15**, 183 (2001).
7. S. Sitch *et al.*, in preparation.
8. P. Bousquet *et al.*, *Science* **290**, 1342 (2000).
9. C. J. Tucker *et al.*, *Int. J. Biometeorol.* **45**, 184 (2001).

10. J. Cihlar *et al.*, *J. Geophys. Res.* **103**, 23163 (1998).
11. G. L. Stenchikov *et al.*, *J. Geophys. Res.* **103**, 13837 (1998).
12. C. Timmreck, H.-F. Graf, I. Kirchner, *J. Geophys. Res.* **104**, 9337 (1999).
13. F. Yang, M. E. Schlesinger, *J. Geophys. Res.* **106**, 14757 (2001).
14. M. L. Roderick, G. D. Farquhar, S. L. Berry, I. R. Noble, *Oecologia* **129**, 21 (2001).
15. J. Conway *et al.*, *J. Geophys. Res.* **99**, 22831 (1994).
16. The cooling effect of the El Chichón volcano eruption in March to April 1982 ($\approx -0.2$ K) was smaller than that of Pinatubo. Only half the amount of $SO_2$ was injected into the stratosphere [S. Self, P. J. Mouginis-Mark, *Rev. Geophys.* **33** suppl. 1, 257 (1995)].
17. A. Menzel, P. Fabian, *Nature* **397**, 659 (1999).
18. P. Y. Groisman, T. R. Karl, R. W. Knight, *Science* **263**, 198 (1994).
19. C. D. Keeling, J. F. S. Chin, T. P. Whorf, *Nature* **382**, 146 (1996).
20. W. Knorr, C. Timmreck, and A. Bondeau have contributed to the interpretation of results; J. Dong and C. J. Tucker were essential to the preparation of the AVHRR data time series; and P. Peylin and P. Ciais contributed to the inversion of atmospheric $CO_2$ observations. The climatology used was produced by the University of East Anglia's Climatic Research Unit. Funding of W.L. by the German Ministry for Education and Research (BMBF) in the DEKLIM program, project CVECA, is gratefully acknowledged. The work of R.B.M. and W.B. was funded by NASA's Earth Science Enterprise.

# Supplemental Material

## Materials and Methods

### Study region

The boreal zone was defined as the region of the northern hemisphere with mean annual temperature < 5ºC and annual precipitation > 200 mm. This zone includes most of Canada, and Eurasia north of a line from southern Norway to northern Korea, plus the Tibetan Plateau. Areas with more than 10%of agricultural land use per quarter degree area as inferred from the USGS Global Land Cover Characterization version 2 data set were masked, eliminating most of Western Europe, the swathe of agricultural lands reaching eastwards from Western Europe, and parts of the western interior of Canada. The remaining area occupies $25.9 \times 10^6$ km$^2$ and represents almost a quarter of the total vegetated land area of the globe.

### Satellite observations

We used the Global Inventory Monitoring and Modeling Systems (GIMMS) Normalized Difference Vegetation Index (NDVI) data set derived from the AVHRR sensors aboard the afternoon-viewing satellite series NOAA 7, 9, 11 and 14, with a spatial resolution of 8 km. Important features of the GIMMS data set relative to

earlier compilations include improved navigation, sensor calibration, and atmospheric correction for stratospheric aerosols (*1, 2*). Residual inconsistencies in the NDVI data after the sensor calibration were addressed by applying a sensor degradation correction method (*3*). Optical effects of stratospheric aerosol loadings due to the eruptions of El Chichón in 1982 and Pinatubo in 1991 were minimized (*4*). Remaining non-vegetation effects in the NDVI data from atmospheric disturbances (for example, clouds) and bidirectional effects, which lower the NDVI, were minimized by analyzing only the maximal NDVI value during each month. These values were used to create an 8 km resolution monthly LAI data set with an algorithm that uses results from a three-dimensional radiative transfer model of radiation scattering in plant canopies (*5*). The relative uncertainties in the satellite-derived LAI fields from the two principal sources of errors, namely uncertainty in the NDVI data and non-uniqueness of the NDVI-LAI relationship, have been estimated (*6*) to vary between 10 and 20%, in agreement with selected comparisons to ground-based determinations of LAI. The LAI data set was finally reduced to 0.5° resolution to match that of the LPJ-DGVM.

**Model**

The Lund-Potsdam-Jena Dynamic Global Vegetation Model (LPJ-DGVM) (*7–10*) was run on a regular latitude-longitude grid at 0.5° resolution. Inputs (by grid cell)

are latitude, soil texture (nine categories), monthly temperature, precipitation and sunshine duration, and annual ambient $CO_2$ concentration. The Farquhar-Collatz photosynthesis scheme (*11, 12*) is coupled to a two-layer hydrological scheme to simulate gross primary production and plant respiration (*13*). Net primary production is allocated annually to four vegetation carbon pools (leaves, sapwood, heartwood, and fine roots) to satisfy allometric relationships, and is redistributed to soil pools with leaf shedding and plant mortality (litter, fast and slow pools). Heterotrophic respiration is a function of soil temperature, moisture and tissue type. A permafrost module simulates active layer dynamics. At each simulated location, several of ten plant functional types may coexist. Their relative proportion is determined by competition among types with different ecological strategies. Intrinsic rates of disturbance by fire are simulated as a function of a threshold litter load and surface soil moisture and temperature. Vegetation structure and composition adjust dynamically to changes in climate so that transient carbon balance phenomena can be simulated at various time scales, including climate-induced tree invasion or dieback as well as the production-respiration balance. The model correctly predicts seasonal cycles of atmospheric $CO_2$ at different latitudes (*7, 10*), the trend in seasonal cycle amplitude (*9*) since the 1960s, interannual variability in the growth rate (*14*) of atmospheric $CO_2$, global patterns of foliage cover and vegetation type (*7, 10*), and seasonal cycles of $CO_2$ and $H_2O$ fluxes and soil moisture content at flux measurement sites (unpublished results). Simulated global net primary productivity

in the 1980s was 69 PgC/yr and net terrestrial biospheric carbon exchange was –0.7 PgC/yr, i.e. a sink of magnitude consistent with $CO_2$-, $O_2$- and $^{13}CO_2$-based budgets of terrestrial and ocean carbon uptake (*15*).

Modeled net ecosystem exchange is influenced by the temperature dependence of plant and soil respiration, about which uncertainty currently remains in all vegetation models. The good agreement of modeled leaf area index anomalies with the satellite observations is evidence that the temperature dependence of the associated modeled net primary production is not inconsistent, while the qualitative agreement of modeled net ecosystem exchange with independent inversion results, also subject to some uncertainty, allows to draw the limited conclusion that the differential response of heterotrophic respiration and net primary production to cooling following the Pinatubo eruption is a reasonable explanation for the post-eruption sink anomaly observed both in the model and in the inversion results.

**Climate data**

We used the 1901-1998 monthly climatology compiled from meteorological data at the Climate Research Unit, University of East Anglia (*16*). A spin-up of 1000 years with invariant mean climate was followed by a 1901-1998 transient run using actual monthly climate.

**LAI Anomalies**

For the LPJ-DGVM, monthly values of the grid cell LAI were computed from the simulated total fraction of radiation absorbed using Beer's law. Area-average anomalies of observed and simulated LAI were formed by area-weighted averaging and subtraction of the multi-year mean. Simulated and observed monthly anomalies were then compared for May to October so as to avoid known problems of the satellite data at low solar angles and in the presence of snow. Annual LAI anomalies are computed as averages over this season. The onset of spring and autumn are defined as the days when a spline interpolation of monthly LAI values achieves one half of the average seasonal amplitude.

**Supplemental Table S1**

**Observed and simulated greening trends at high latitudes**

| **Linear Fits to Time Series** | | **Change in timing (days)** | | **Maximal LAI (ratio LPJ/Sat)** |
|---|---|---|---|---|
| | | **Spring** | **Autumn** | |
| Satellite | before Pinatubo 1982-1991 | − 8 | + 8 | + 0.23 |
| | after Pinatubo 1991-1998 | − 5 | + 13 | + 0.33 |
| | complete period 1982-1998 | − 7 | + 8 | + 0.19 |
| | change in 1991 | + 4 | − 9 | − 0.27 |
| Satellite vs. LPJ | linear correlation | 0.91 | (0.48) | 0.73 |
| LPJ vegetation model | before Pinatubo 1982-1991 | − 6 | + 2 | + 0.15 (65%) |
| | after Pinatubo 1991-1998 | − 2 | + 5 | + 0.28 (85%) |
| | complete period 1982-1998 | − 4 | + 2 | + 0.12 (63%) |
| | change in 1991 | + 3 | − 4 | − 0.22 (81%) |

Values reflect linear fits to growing season (May-October) values. Correlation coefficient in parentheses is not significant, $P > 0.05$. Percentages given are with respect to the satellite data.

**References and Notes**

1. G. W. Rosborough, D. G. Baldwin, W. J. Emery, *IEEE Trans Geosci. Remote Sens.* **32**, 644 (1994).

2. E. F. Vermote, Y. J. Kaufman, *Int. J. Remote Sens.* **16**, 2317 (1995).

3. S. O. Los, IEEE Trans. Geosci. Remote Sens. **36**, 202 (1998).

4. E. F. Vermote, N. Z. El Saleous, *Atmos. Sens. Mod.* **2311**, 19 (1994).

5. R. B. Myneni, R. R. Nemani, S. W. Running, *IEEE Trans. Geosci. Remote Sens.* **35**, 1380 (1997).

6. W. Buermann *et al.*, *J. Geophys. Res.* in press.

7. S. Sitch, dissertation, Lund University, Sweden (2000).

8. W. Cramer *et al.*, *Global Change Biol.* **7**, 357 (2001).

9. D. McGuire *et al.*, *Global Biogeochem. Cycles* **15**, 183 (2001).

10. S. Sitch *et al.*, in preparation.

11. G. D. Farquhar, S. von Caemmerer, J. A. Berry, *Planta* **149**, 78 (1980).

12. G. J. Collatz, M. Ribas-Carbo, J. A. Berry, *Austral. J. Plant Physiol.* **19**, 519 (1992).

13. Haxeltine, A., I. C. Prentice, *Global Biogeochem. Cycl.* **10**, 693 (1996).

14. C. Prentice, M. Heimann, S. Sitch, *Ecol. Appl.* **10**, 1553 (2000).

15. C. Prentice et al., in Climate Change 2001: The Scientific Basis. Contribution of Working Group I to the Third Assessment Report of the Intergovernmental

Panel on Climate Change, J. T. Houghton et al., Eds. (Cambridge Univ. Press, Cambridge, MA, 2001), pp. 183-237.

16. M. G. New, M. Hulme, P. D. Jones, *J. Clim.* **13**, 2217 (2000).